

# A new multibeam receiver for KOSMA with scalable fully reflective focal plane array optics

T. Lüthi\*, D. Rabanus\*, U. U. Graf\*, C. Granet<sup>†</sup> and A. Murk<sup>‡</sup>

\*KOSMA, I. Physikalisches Institut, Universität zu Köln, Zùlpicher Strasse 77, 50937 Köln, Germany

Email: luethi@ph1.uni-koeln.de

<sup>†</sup>CSIRO ICT Centre, PO Box 76, Epping NSW 1710, Australia

<sup>‡</sup>Institute of Applied Physics, Universität Bern, Sidlerstrasse 5, 3012 Bern, Switzerland

**Abstract**— We are developing a new submillimeter heterodyne array receiver for the KOSMA 3m telescope on Gornergrat, Switzerland. In order to facilitate assembly and maintenance, the receiver consists of two self-contained 3×3 beam cartridge-type receiver modules. They employ new focal plane array optics which are both fully reflective and scalable in frequency as well as in the number of beams. So far, a first 345 GHz focal plane array optics prototype has been realized and its near field patterns have been measured.

We describe the overall receiver design and present the focal plane array optics as well as the measured focal plane beam patterns.

## I. INTRODUCTION

Heterodyne multibeam receivers greatly improve the mapping performance of millimeter and submillimeter telescopes. As the noise temperature of single-beam receivers approaches the quantum limit, a further increase in mapping speed requires multibeam receivers. However, there should be made no compromises resulting in an increased noise temperature of the individual receiver channels. The mapping time for a given area and a desired sensitivity increases with the square of the receiver noise temperature, but decreases only linearly with the number of receivers.

Today, there already exist several operational heterodyne array receivers at short millimeter and submillimeter wavelengths (e.g. SMART [1], HERA [2], PoleSTAR [3]). SMART is a dual-frequency/eight-beam receiver operating at 490 and 810 GHz, used as a facility instrument at the KOSMA 3m telescope on Gornergrat, Switzerland [4]. In order to replace the telescope's older 230/345 GHz dual-frequency/single-beam receiver, we are developing a 2×9 beam array receiver. It is based on two self-contained 3×3 beam cartridge-type receiver modules [5]. The modular receiver design not only facilitates assembly and maintenance, it also allows a rapid adaptation to the seasonal observation conditions. For the dry winter months the receiver modules can be easily replaced with higher-frequency units.

The receiver modules employ a new focal plane array optics which is fully reflective, thus avoiding the absorption and reflection losses of dielectric lenses. It is scalable both in frequency as well as – for the first time with a fully reflective array – to an arbitrary number of beams. So far, a first 345 GHz focal plane array optics prototype has been realized and its near field patterns have been measured.

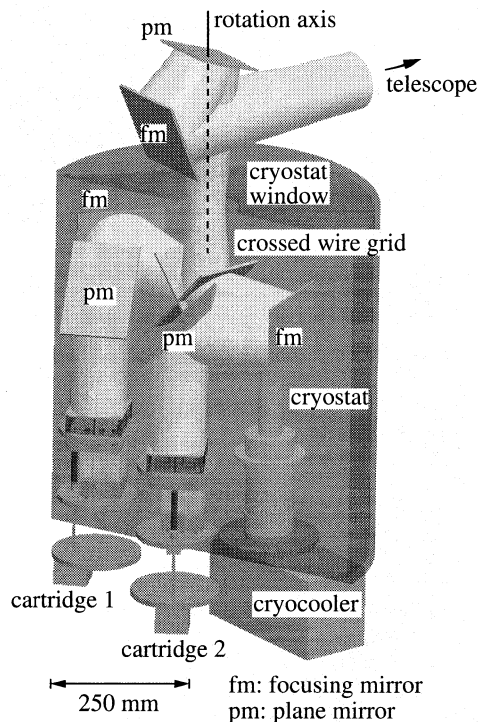


Fig. 1. General layout of the array receiver. The cryostat uses a two-stage cryocooler (50 and 4 K). Not shown are the inner radiation shields, thermal links and the support structure. The indicated beam contour is the envelope of all nine beams at 345 GHz.

In this paper we describe the overall receiver design and present the focal plane array optics and the first measured focal plane beam patterns.

## II. RECEIVER OVERVIEW

In order to fit into the limited space available at the KOSMA 3m telescope the instrument has to be very compact. A general overview of the receiver layout is shown in Fig. 1. The telescope focal plane is re-imaged by a Gaussian telescope into the cryostat, with a pupil at the location of the cryostat window in order to minimize the window size. The warm optics consist of two mirrors (one focusing and one plane mirror) mounted at the telescope's Nasmyth port.

Inside the cryostat the telescope signal is split into two orthogonal polarizations by crossed wire grids, followed by

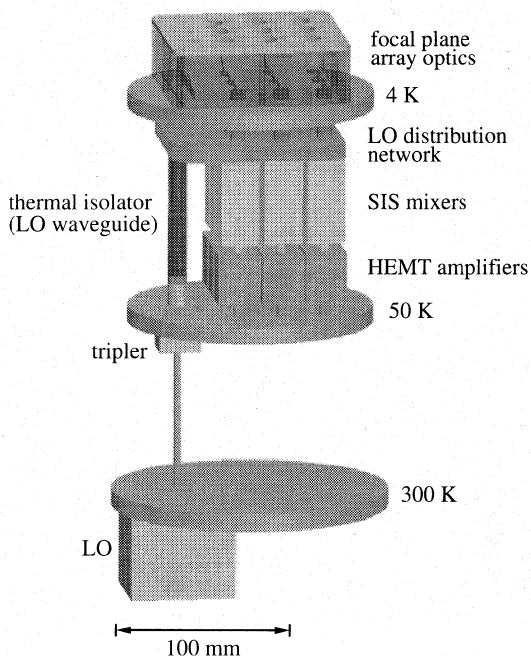


Fig. 2. General layout of the receiver modules. Not shown are the IF/DC cables and the cartridge support structure.

the second focusing mirror of the Gaussian telescope and a further plane mirror. Finally, the beams are coupled through two focal plane array optics into the individual feedhorns. This folded optics design allows a very compact optical layout.

Image de-rotation will be accomplished by a rotating cryostat (e.g. [6]), thus eliminating the need for an external image rotator. However, this leads to a varying relative alignment of the focusing off-axis mirrors of the Gaussian telescope. Therefore the two focusing mirrors will have to be optimized in order to minimize the resulting aberrations [2].

The cryostat houses two self-contained  $3 \times 3$  beam cartridge-type receiver modules. The cartridge concept with automatic thermal link was introduced for the ALMA receivers [5], [7] and is also highly advantageous for array receivers. Assembly and maintenance are facilitated considerably, and the receiver modules are easily replaced in order to adapt to seasonal observation conditions.

Each module (Fig. 2) consists of the focal plane optics, feedhorns, sideband-separating SIS-mixers, HEMT-amplifiers and local oscillator. The local oscillator will be a synthesizer/multiplier chain at ambient temperature, with the final tripler at cryogenic temperature (50 K). Thermal isolation of the LO-waveguide between the 50 and 4 K stage will be accomplished either by a microwave bandgap joint [8] or two face-to-face feedhorns. The LO distribution network to the nine mixers will be realized entirely in waveguide technology, which allows a compact optical design as no quasioptical diplexer is required.

### III. FOCAL PLANE ARRAY OPTICS

The focal plane optics match the beams of the feedhorns to those provided by the telescope. They should have low loss

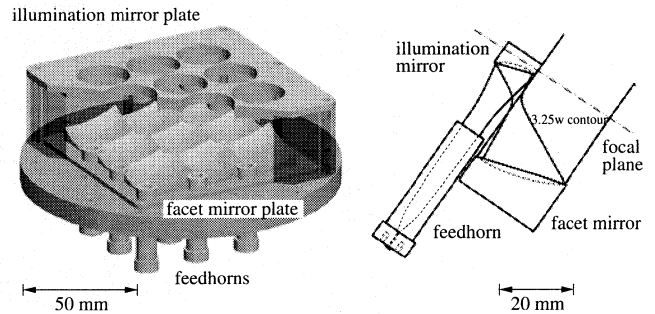


Fig. 3.  $3 \times 3$  beam focal plane array optics (left) and optics unit-cell with the  $3.25 w$  beam contour (right). Aside from the feedhorns the focal plane array optics consists of only three major parts: two plates with all the facet and illumination mirrors, respectively, and a spacer frame.

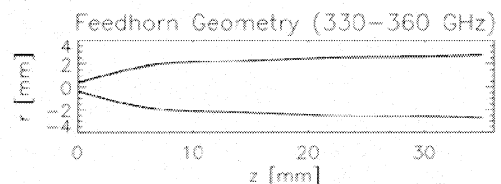


Fig. 4. Optimized feedhorn profile for the 330–360 GHz band.

and be compact in order to match the space requirements of a cartridge-type receiver module. In order to avoid the absorption and reflection losses of dielectric lenses, it is desirable to use fully reflective optics. However, fully reflective array receivers so far offered a maximum of four rows of beams per optics module, as they used feedhorns located beside their individual off-axis mirrors (e.g. [1], [9]). In our setup, however, the beams are arranged on a rectangular grid, with the feedhorns and small illumination mirrors located in the gaps between the individual beams (Fig. 3 left). Thus, for the first time with fully reflective optics, the array is scalable to an arbitrary number of beams.

The optics unit-cell (Fig. 3 right) consists of the feedhorn ( $w_0=1.8$  mm) and the elliptical illumination and facet mirrors ( $f=7.4$  and  $21.2$  mm, respectively). The reflection angles are  $35^\circ$ . As the illumination mirror is located at only  $\sim$ one third of the far-field distance  $2D^2/\lambda$  from the feedhorn, the latter, a smooth-walled spline-profile feedhorn, is optimized to produce a Gaussian beam on the illumination mirror, 22 mm in front of its aperture. The optimization method [10] varies the spline-profile, computes the resulting beam pattern via a mode-matching algorithm and compares it to the pattern to be met. Thus, feedhorns can be customized for a wide range of applications. Additionally, the smooth-walled feedhorns can be manufactured considerably easier than corrugated ones, which is an important cost-saving factor for array receivers that use large numbers of feedhorns. The optimized feedhorn profile for the 330–360 GHz band is shown in Figure 4.

As a compromise between a short mapping time and high complexity we have chosen a  $3 \times 3$  beam arrangement. Additionally, this provides a center pixel to facilitate pointing, and the rectangular beam arrangement allows efficient on-the-fly

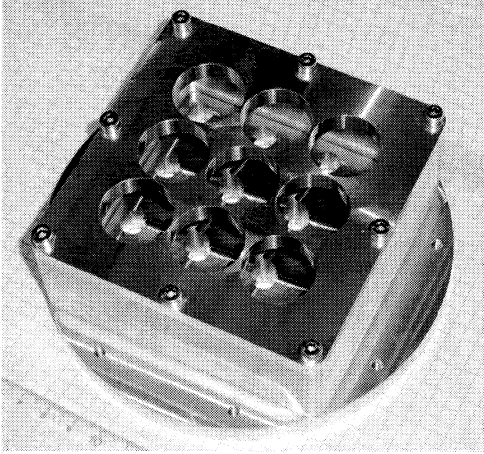


Fig. 5. 345 GHz focal plane array optics prototype.

mapping (equidistant sampling when the array is inclined by 18.4 deg with respect to the scanning direction, [2]).

In order to minimize the need for optical alignment, large optical sub-assemblies are machined monolithically, using CNC milling techniques. Aside from the feedhorns, the focal plane optics consist therefore of only three major parts: two plates with all the facet and illumination mirrors, respectively, and a spacer frame.

The focal plane array optics were designed using a 3D-CAD software (*Pro/Engineer Wildfire*) and simulated with a physical optics beam propagation software [11]. In order to check the design, a first 345 GHz prototype has been built (Fig. 5) and its focal plane beam patterns have been measured.

#### IV. MEASUREMENTS

Both the feedhorn and focal plane patterns were measured in amplitude and phase with a scanning vector network analyzer from *AB-Millimetre*. The signal-to-noise ratio was 50–60 dB. We obtained 1D scans at 330, 345 and 360 GHz, as well as 2D scans at 345 GHz. All scans were repeated with the probes moved  $\lambda/4$  away from the device under test, in order to correct for standing waves.

From the measured amplitude and phase the parameters of the best fitting Gaussian beam were obtained by maximizing the coupling integral of the measured beam pattern to a fundamental mode Gaussian. We thus obtained the waist radius  $w_0$  and location  $z$ , as well as lateral and pointing offsets of the measured beams.

##### A. Feedhorn

Angular cuts of the feedhorn radiation pattern (far field) were obtained by rotating the feedhorn around its calculated phase center. The 345 GHz radiation pattern is shown in Figure 6: In H-plane, the agreement between the measurement (bold curves) and the simulation (thin curves) is excellent. In E-plane, we measure a slightly increased side-lobe level. Cross polarization (D-plane) is also slightly higher than simulated. A similar behavior is also observed at 330 and 360 GHz, with

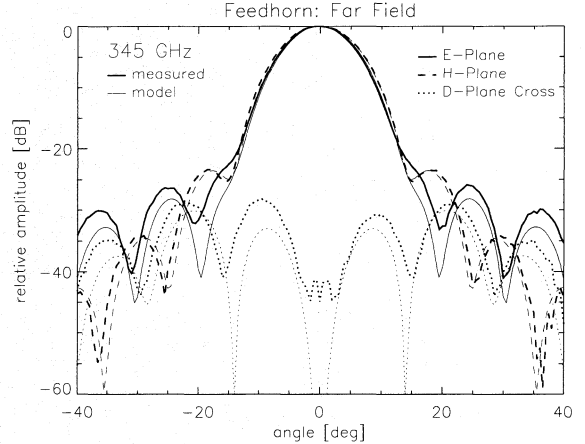


Fig. 6. E- and H-plane co-polar, and D-plane (45°) cross-polar radiation pattern of the feedhorn at 345 GHz. Bold curves: measurements, thin curves: simulation.

the best agreement between measurements and simulations at 330 GHz. The far-field cuts clearly show that the feedhorn works as specified down to -20 dB over the whole bandwidth of 330–360 GHz, and is well suited for use in our focal plane array optics.

At 345 GHz, we also measured the near field radiation pattern in the plane of the illumination mirror, 22 mm in front of the feedhorn aperture. These measurements were obtained with a rectangular waveguide-probe (0.4 mm×0.8 mm) on a planar xy-scanner. Again, measurements and simulation agree well, and we find  $w_0=1.8$  mm. The waist is located 2.8 mm *outside* the aperture plane (simulation: 2.6 mm), which opens the possibility to use two of these feedhorns also as a thermal isolator for the LO-waveguide. As the waist is located outside the feedhorn, two of them can be joined face-to-face with a 5.6 mm gap in between. The alignment requirements of two coupling Gaussian beams are much less stringent than those of a microwave bandgap joint [8]. However, we still have to evaluate the effect of the slightly changing waist location with frequency, as well as possible resonances of higher order modes [12].

##### B. Focal Plane Array Optics

The E-plane of the feedhorn is inclined by 45 deg with respect to the unit-cell's symmetry plane (y-plane in Fig. 7 left). This orientation is best suited for the subsequent mounting of the mixer blocks and the LO-distribution network.

We obtained 1D scans at 330, 345 and 360 GHz of the center beam (1), as well as 2D scans of the center and a corner beam (2) at 345 GHz. All these measurements were made in the near field with a planar scanner 100 mm in front of the array focal plane.

The 2D patterns of both measured beams agree well down to the -40 dB level. The power pattern of the center beam is shown in Figure 7. It corresponds well to a Gaussian down to the -20 dB level, below which is a slight asymmetry in

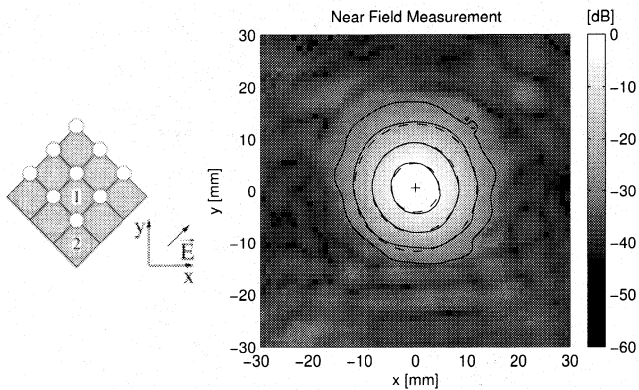


Fig. 7. Coordinate system for the focal plane array measurements (left) and center beam power pattern measured 100 mm in front of the array focal plane. The contour levels are -3, -10, -20 and -30 dB. Also shown is the center (+) and the contours (dashed lines) of the best fitting Gaussian beam.

y-direction (i.e. the asymmetric direction of the optics unit-cell). The X-shaped structure at the -40 dB level is due to the basically square shape of the facet mirrors, truncating the beam at  $\geq 3.25 w$ . From the best fit to a Gaussian beam (dashed) we obtain  $w_0=7.0$  mm with an asymmetry between the x- and y-direction of  $\sim 3.6\%$  and a Gaussicity  $\geq 98\%$ . The focal plane beam separation is thus  $\sim 3.6 w_0$ , which translates into  $\sim 2.3$  HPBW on the sky. The linear scans at the other frequencies yield beam waists of 7.4 and 6.7 mm at 330 and 360 GHz, respectively. Thus, the beam waist scales well with the wavelength.

Linear cuts of the center beam at 345 GHz are shown in Figure 8. Cross-polarization is well below -25 dB. Also indicated is the simulated co-polar power pattern, which is slightly broader than measured. Indeed, the measured beam waist of 7.0 mm is slightly less than simulated ( $\sim 7.2$  mm). This difference does not affect the functionality of the focal plane array optics. However, simulations indicate that it might be due to an alignment error between the illumination and facet mirror plates. If this can be confirmed by mechanical sampling of the mirror surfaces, it will be easily corrected by a modified spacer frame. The array should then reach its nominal performance with a beam separation of  $3.4 w_0$  in the focal plane, corresponding to  $\sim 2.2$  HPBW on the sky.

## V. CONCLUSIONS

We are developing a new submillimeter array receiver for the KOSMA telescope, based on cartridge-type receiver modules. The receiver modules employ new fully reflective focal plane array optics, thus avoiding the absorption and reflection losses of dielectric lenses. They are scalable both in frequency and – for the first time with a fully reflective array – to an arbitrary number of beams. A 345 GHz  $3 \times 3$  beam optics prototype was built and successfully tested. The measured focal plane beams exhibit a Gaussicity of  $\geq 98\%$  and best fit a Gaussian beam with a waist radius  $w_0$  of 7.0 mm at 345 GHz. This corresponds to a focal plane beam separation of  $2.6 w_0$ , or 2.3 HPBW on the sky.

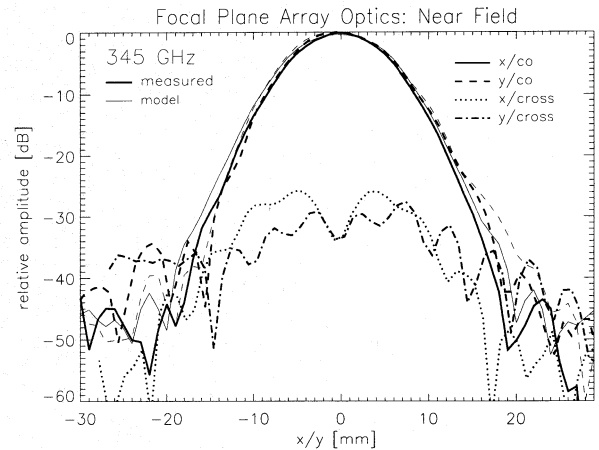


Fig. 8. Linear cuts along the x- and y-plane of the 345 GHz power pattern. Bold curves: measurements, thin curves: simulation (only shown for co-polarization).

## ACKNOWLEDGMENTS

This research is supported by Swiss National Science Foundation under grants PBBE2-106793 and 200020-100167, Deutsche Forschungsgemeinschaft under grant SFB 494, and by the ministry of science of the state Nordrhein-Westfalen.

## REFERENCES

- [1] U. U. Graf, S. Heyminck, E. A. Michael, S. Stanko, C. E. Honingh, K. Jacobs, R. Schieder, and J. Stutzki, "SMART: The KOSMA Sub-Millimeter Array Receiver for Two frequencies," in *Thirteenth International Symposium on Space Terahertz Technology*, vol. 4855. Harvard University, Mar. 2002, pp. 143–152.
- [2] K.-F. Schuster, C. Boucher, W. Brunswig et al., "A 230 GHz heterodyne receiver array for the IRAM 30 m telescope," *A&A*, vol. 423, pp. 1171–1177, Sept. 2004.
- [3] C. Walker, C. Groppi, D. Golish et al., "PoleStar: An 810 GHz Array Receiver for AST/RO," in *Proceedings of the 12<sup>th</sup> International Symposium on Space Terahertz Technology*, 2001, pp. 540–552.
- [4] C. Kramer, C. G. Degiacomi, U. U. Graf, R. E. Hills, M. Miller, R. Schieder, N. Schneider, J. Stutzki, and G. Winnewisser, "The new KOSMA 3m telescope," in *Proc. SPIE*, vol. 3357, 1998, pp. 711–720.
- [5] W. Wild, J. Payne, J. W. Lamb et al., ALMA Project Book, Chapter 5, Tech. Rep., 2002.
- [6] R. Güsten, G. Ediss, F. Gueth et al., "CHAMP – The Carbon Heterodyne Array of the MPIfR," in *Proc. SPIE*, vol. 3357, Mar. 1998, pp. 167–177.
- [7] A. Orłowska, M. Harman, and B. Ellison, ALMA Project Book, Chapter 6, Tech. Rep., 2001.
- [8] J. L. Hesler and N. Horner, "A Broadband Waveguide Thermal Isolator," *ALMA memo 469*, Tech. Rep., 2003.
- [9] D. Rabanus, U. Graf, M. Philipp, J. Stutzki, and A. Wagner, "Cryogenic Design of KOSMA's SOFIA Terahertz Array Receiver (STAR)," *SPIE: Airborne Telescope Systems*, vol. 5498, pp. 473–480, 2004.
- [10] C. Granet, G. L. James, R. Bolton, and G. Moorey, "A Smooth-Walled Spline-Profile Horn as an Alternative to the Corrugated Horn for Wide Band Millimeter-Wave Applications," *IEEE Transactions on Antennas and Propagation*, vol. 52, pp. 848–854, Mar. 2004.
- [11] S. Heyminck, "Entwicklung und Test von optimierten Phasengittern für Submillimeter Mehrkanal-Empfänger," Master's thesis, I. Physikalisches Institut, Universität zu Köln, 1999.
- [12] W. Jellema, S. Withington, N. Trappe, J. A. Murphy, and W. Wild, "Theoretical and Experimental Study of High-Q Resonant Modes in Terahertz Optical Systems," in *Joint 29<sup>th</sup> International Conference on Infrared and Millimeter Waves and 12<sup>th</sup> International Conference on Terahertz Electronics*, 2004, pp. 805–806.